

Synthesis and Structural, Redox and Photophysical Properties of Tris-(2,5-di(2-pyridyl)pyrrolide) Lanthanide Complexes

James N. McPherson,^a Laura Abad Galan,^b Hasti Iranmanesh,^a Max Massi^{b*} and Stephen B. Colbran^{a*}

^aSchool of Chemistry, University of New South Wales, NSW 2052 Australia;

^bDepartment of Chemistry, Curtin University, WA 6102 Australia

Electronic Supplementary Information

SC-XRD structures

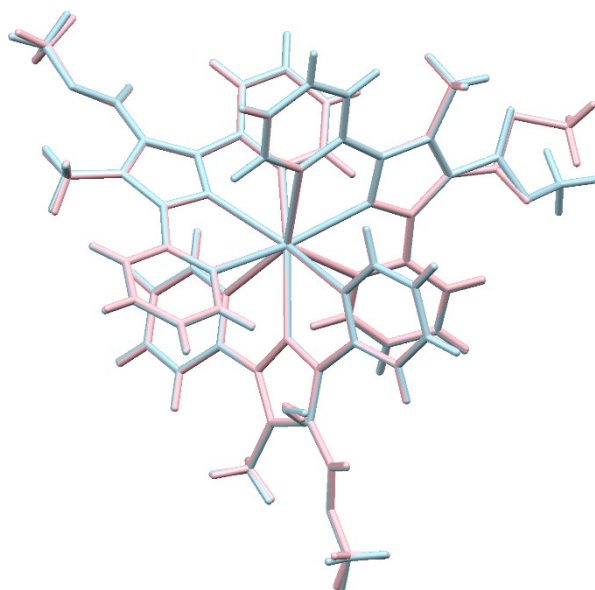


Fig S1. Overlaid SC-XRD structures of [Sm(dpp^{CO₂Me,Me})₃] (pink) and [Eu(dpp^{CO₂Me,Me})₃] (light blue) by matching the Ln(III) centre and 9 coordinating N atoms (RMSD = 0.0119 Å).

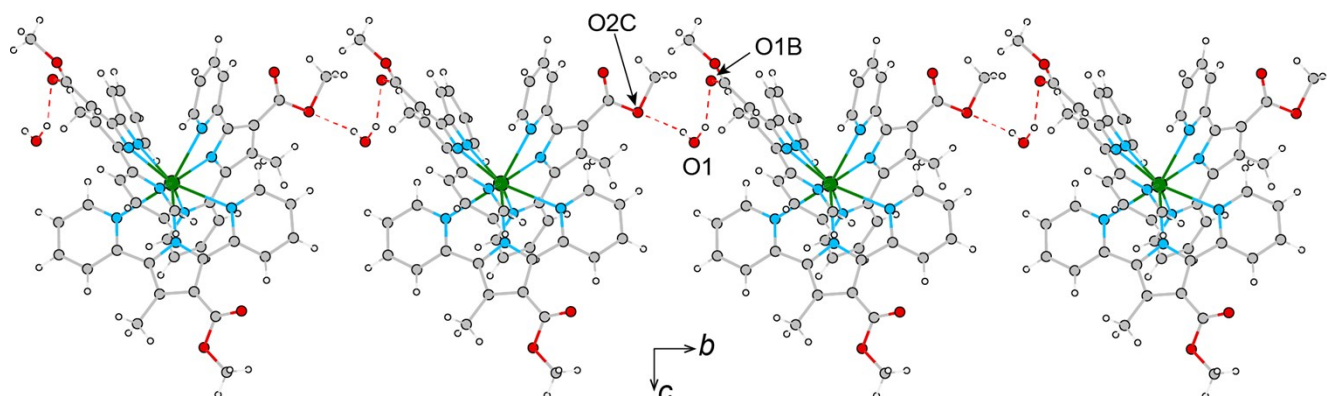


Fig S2. H-bonding network with the lattice water molecule linking neighbouring [Ln(dpp^{CO₂Me,Me})₃] complex molecules (Ln = Sm, Eu) down the *b* axis. Key distances and angles: Ln = Sm: O2C...O1 2.90(1) Å, O1...O1B 2.91(1) Å, and O2C–O1–O1B 92.8(4); Ln = Eu: O1C'...O1 2.91(3) Å, O1...O1B 2.92(2) Å, and O1C'–O1–O1B 98.3(7)°.

Table S1. Experimental details

Complex	[La(dpp ^{Me,Me}) ₃]	[Sm(dpp ^{CO₂Me,Me}) ₃]	[Eu(dpp ^{CO₂Me,Me}) ₃]
CIF name	p1bar_a	james_sm1_a	James_Eu_June18_0m_a
Crystal data			
Chemical formula	C ₄₈ H ₄₂ LaN ₉ ·1.5(C ₆ H ₆)	2(C ₅₁ H ₄₂ N ₉ O ₆ Sm)·H ₂ O	C ₅₁ H ₄₂ EuN ₉ O ₆ ·0.5(H ₂ O)
<i>M</i> _r	1000.98	2072.58	1066.48
Crystal system, space group	Triclinic, <i>P</i> ⁻ 1	Monoclinic, <i>P</i> 2 ₁ / <i>n</i>	Monoclinic, <i>P</i> 2 ₁ / <i>n</i>
Temperature (K)	100	100	99.95
<i>a</i> , <i>b</i> , <i>c</i> (Å)	12.928 (3), 13.980 (3), 14.100 (3)	17.177 (3), 13.222 (3), 19.402 (4)	17.3254(12), 13.3245(9), 19.4895(13)
α, β, γ (°)	80.97 (3), 83.88 (3), 70.72 (3)	90.85 (3)	90.717(2)
<i>V</i> (Å ³)	2371.5 (9)	4406.0 (15)	4498.8(5)
<i>Z</i>	2	2	4
Radiation type	Mo <i>K</i> α	Mo <i>K</i> α	Mo <i>K</i> □
μ (mm ⁻¹)	0.95	1.40	1.458
Crystal size (mm)	0.02 × 0.01 × 0.01	0.02 × 0.02 × 0.02	0.1 × 0.04 × 0.01
Data collection			
Diffractometer	ADSC Quantum 210r	ADSC Quantum 210r	Bruker D8 Quest
Absorption correction	–	–	SADABS
No. of measured, independent and observed [<i>I</i> > 2σ(<i>I</i>)] reflections	39500, 10228, 9722	65218, 9559, 8469	146595, 7935
<i>R</i> _{int}	0.018	0.029	0.1555
(sin θ/λ) _{max} (Å ⁻¹)	0.658	0.641	0.595
Refinement			
<i>R</i> [<i>F</i> ² > 2σ(<i>F</i> ²)], <i>wR</i> (<i>F</i> ²), <i>S</i>	0.024, 0.061, 1.07	0.039, 0.103, 1.14	0.0479, 0.1249, 1.076
No. of reflections	10228	9559	7935
No. of parameters	611	651	653
No. of restraints	–	11	49
H-atom treatment	H-atom parameters constrained	H-atom parameters constrained	H-atom parameters constrained
Δ _{max} , Δ _{min} (e Å ⁻³)	0.51, -1.40	0.92, -1.16	0.94, -0.85

Computer programs: Blucce (McPhillips, 2002), XDS (Kabsch, 1993), *SHELXT* (Sheldrick, 2015), *SHELXL* (Sheldrick, 2015), Olex2 (Dolomanov *et al.*, 2009).

NMR Spectra

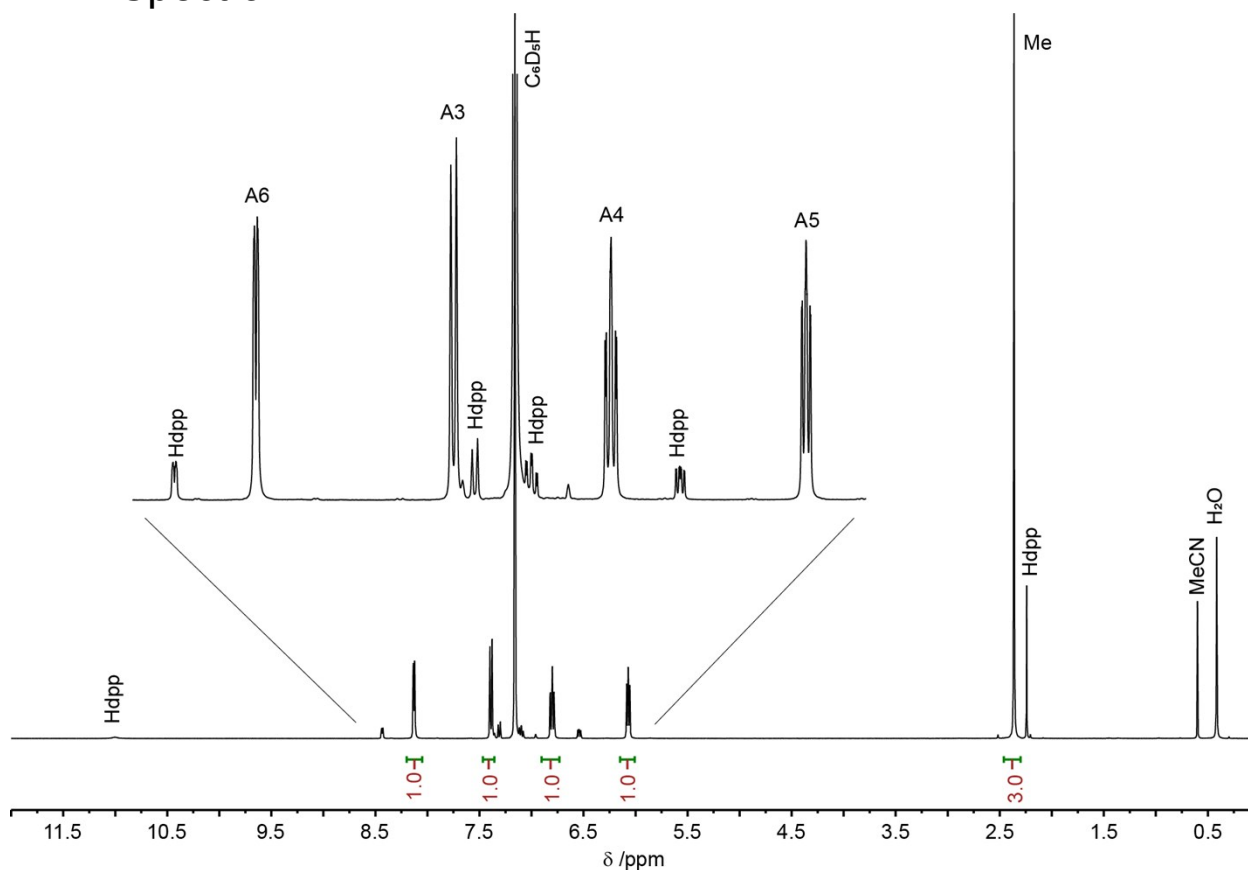


Fig. S3. ^1H NMR (400 MHz, C_6D_6) spectrum of $[\text{La}(\text{Me},\text{Me-dpp})_3]$.

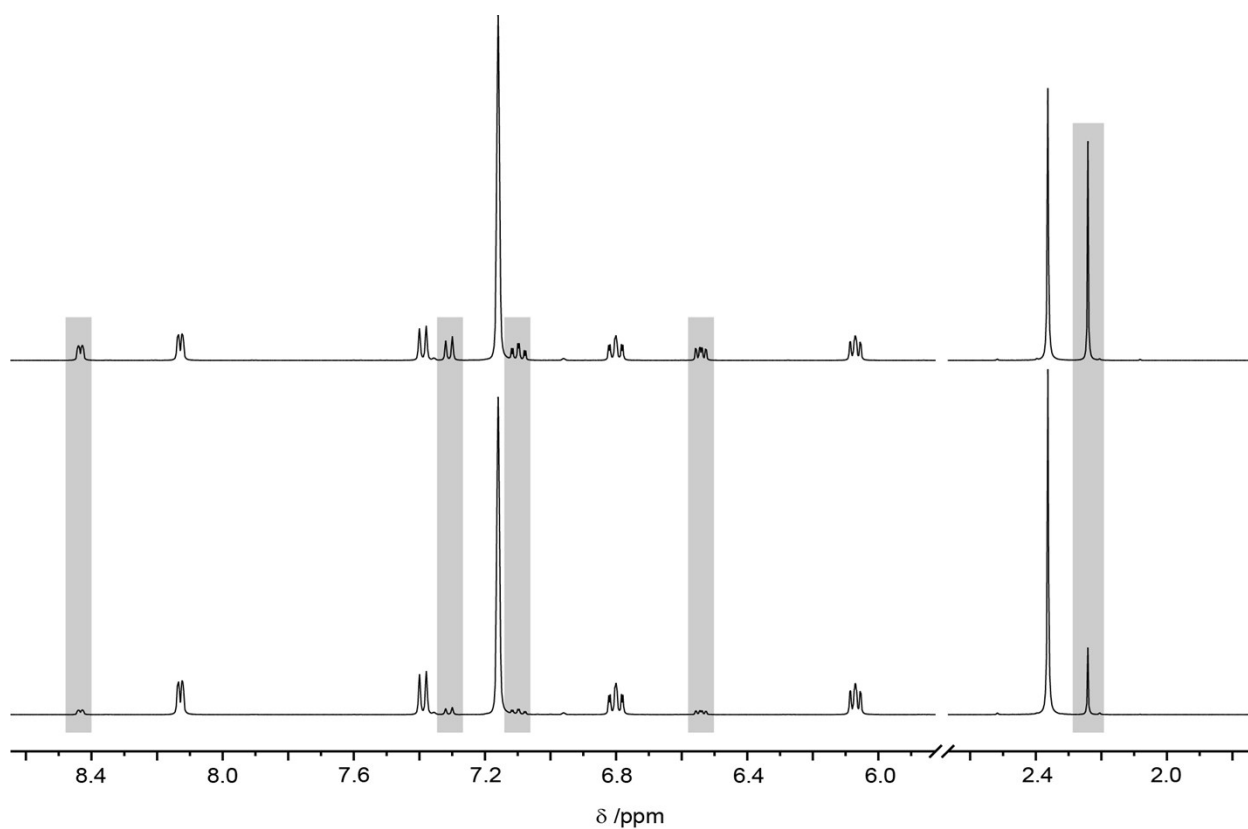


Fig. S4. ^1H NMR (400 MHz, C_6D_6) spectra of $[\text{La}(\text{dpp}^{\text{Me},\text{Me}})_3]$: after 20 minutes in solution (bottom) and after 6 hours in solution (top). The signals, which correspond to unbound $\text{dpp}^{\text{Me},\text{Me}}\text{H}$ —and increase over time—have been highlighted by grey regions.

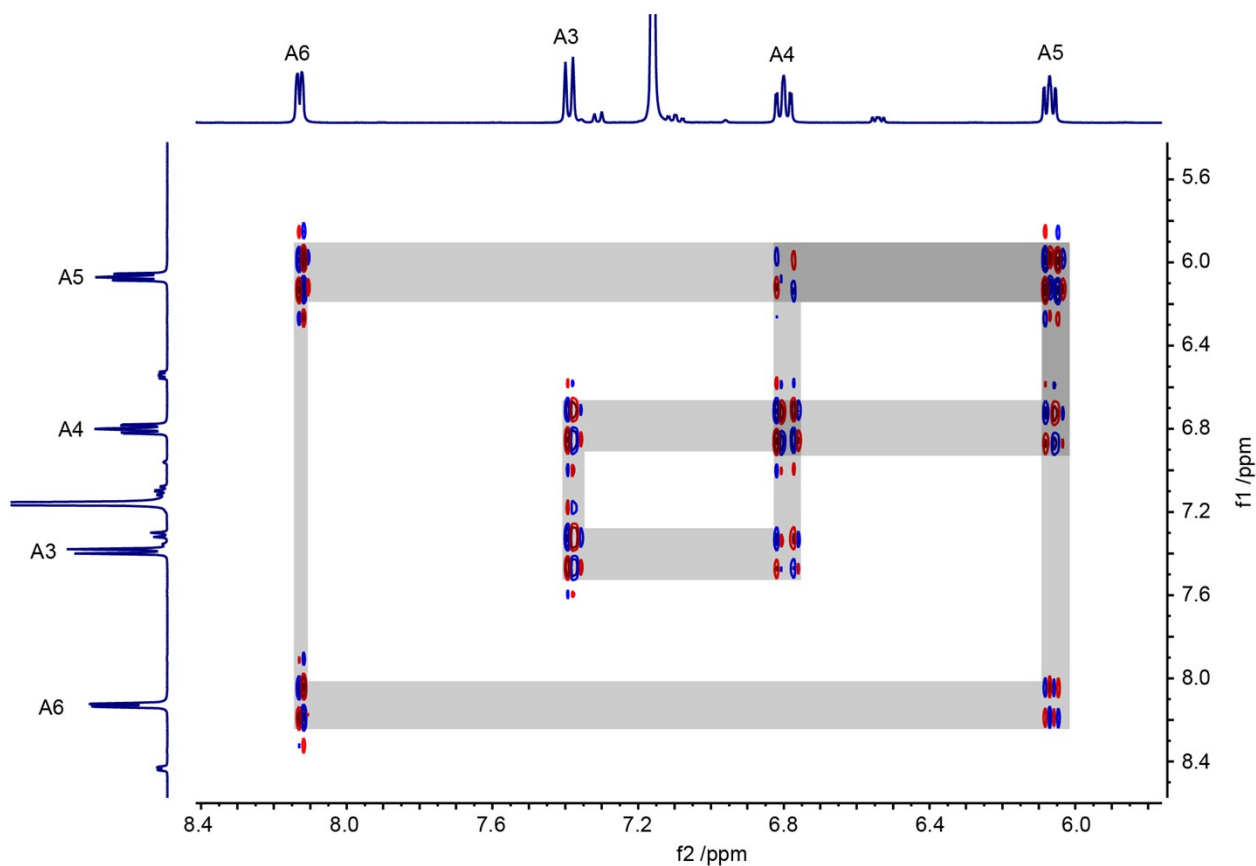


Fig S5. ^1H - ^1H COSY NMR (400 MHz, C_6D_6) spectrum of $[\text{La}^{(\text{Me},\text{Me})\text{dpp}}]_3$.

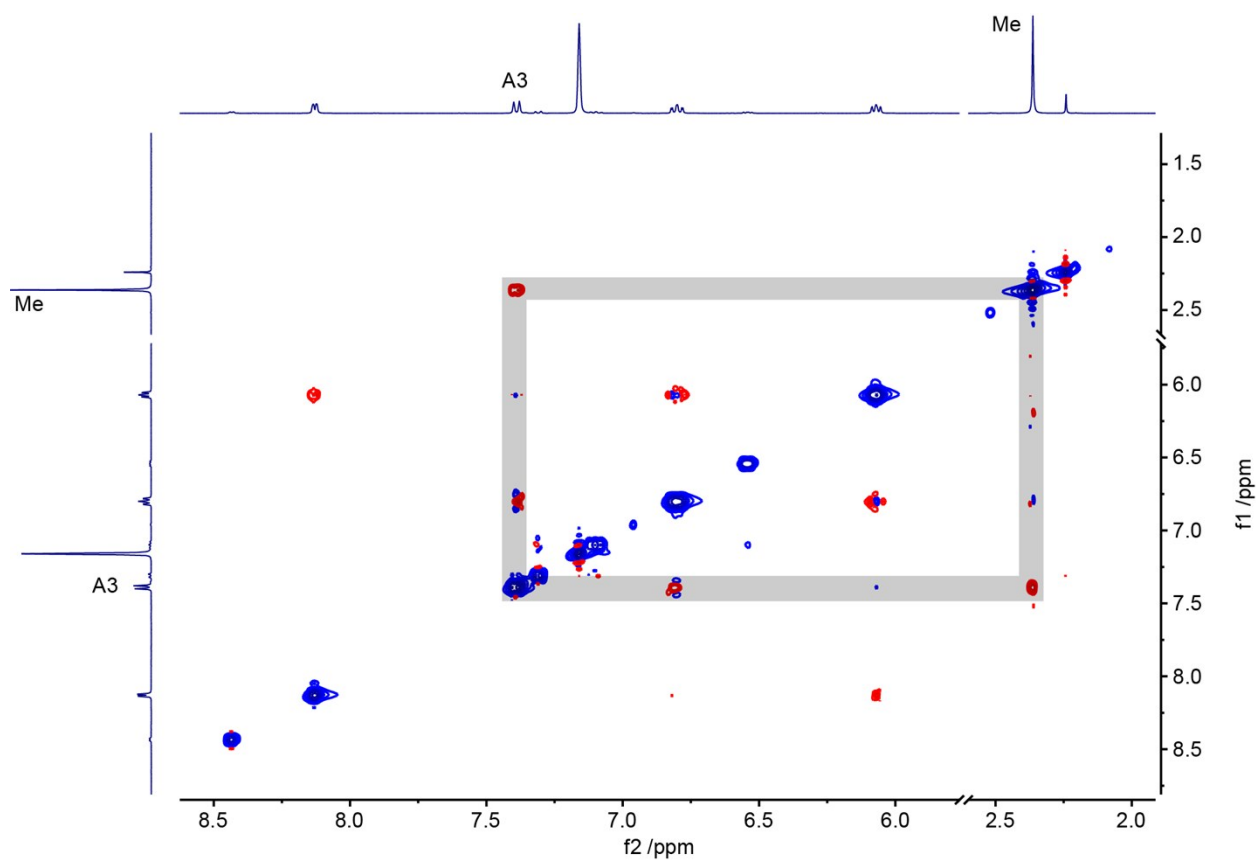


Fig S6. ^1H - ^1H nOeSY NMR (400 MHz, C_6D_6) spectrum of $[\text{La}^{(\text{Me},\text{Me})\text{dpp}}]_3$. The key interaction (A3 – Me) has been highlighted.

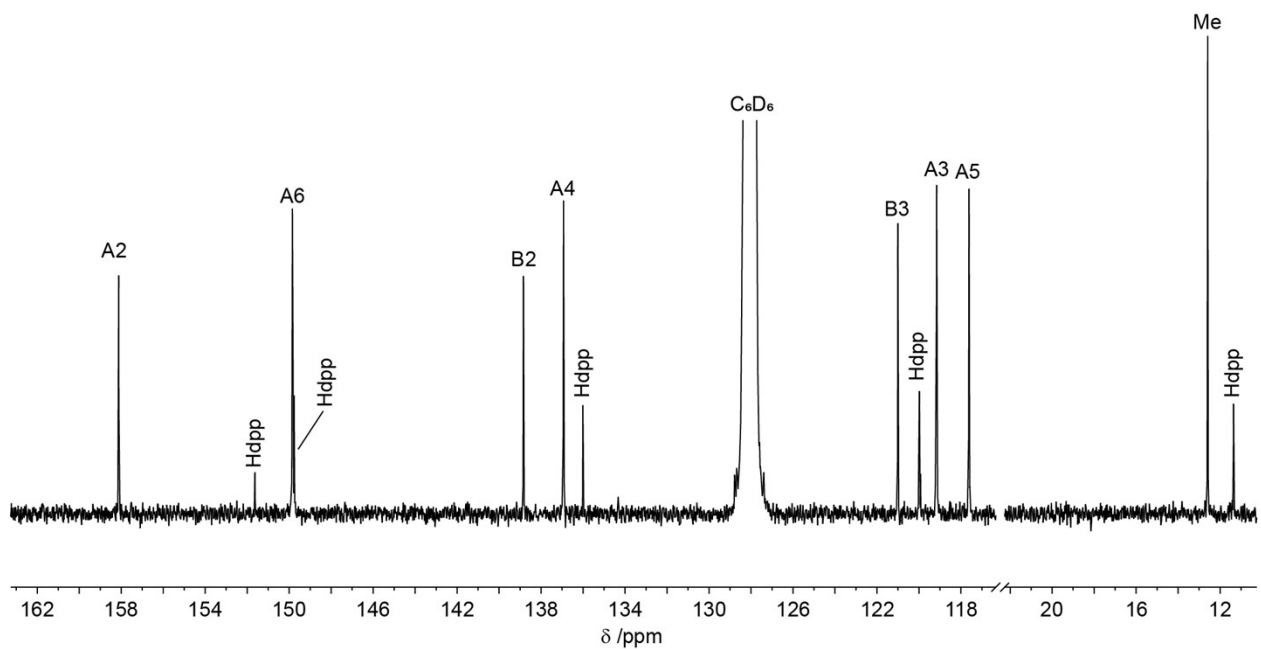


Fig. S7. $^{13}\text{C}\{^1\text{H}\}$ NMR (101 MHz, C_6D_6) spectrum of $[\text{La}^{(\text{Me,Me dpp})}_3]$.

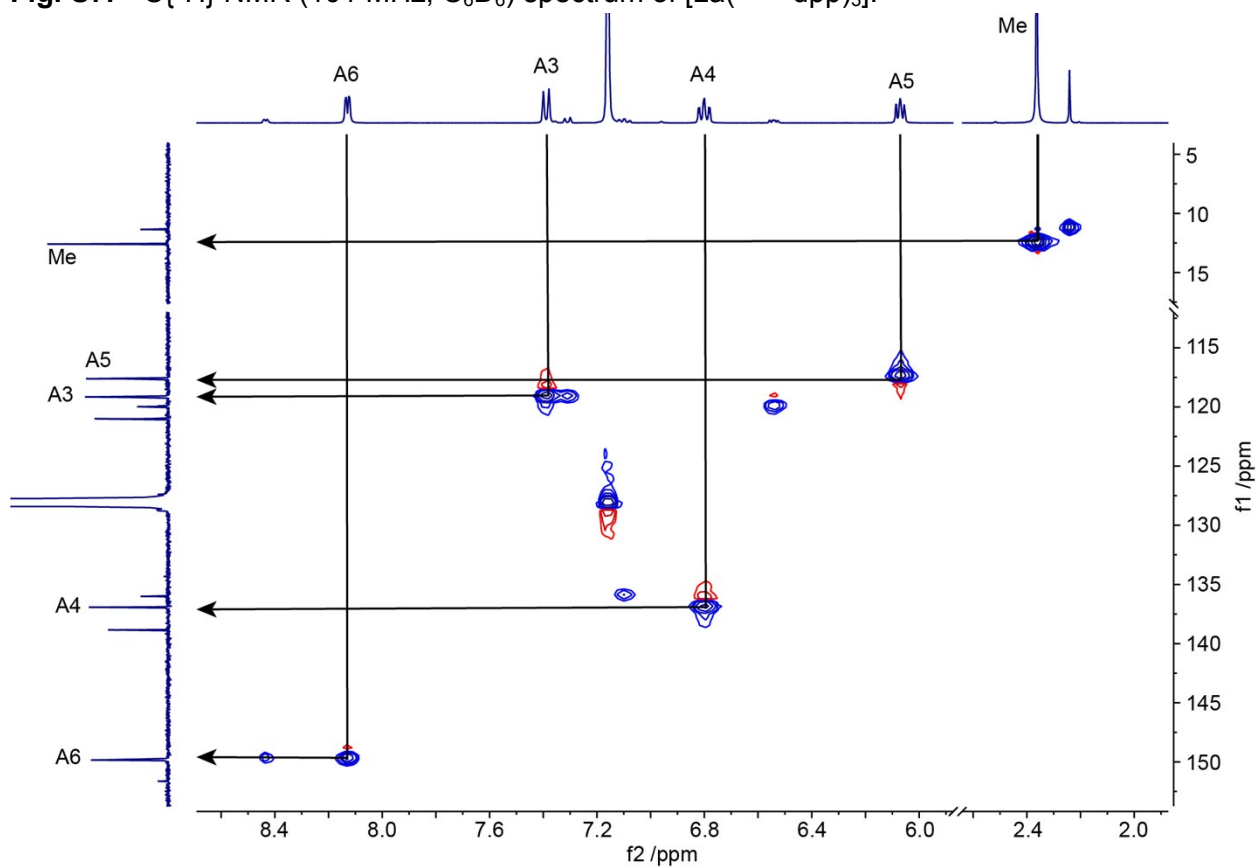


Fig S8. $^1\text{H}\text{-}^{13}\text{C}\{^1\text{H}\}$ HSQC NMR (400 MHz, 101 MHz, C_6D_6) spectrum of $[\text{La}^{(\text{Me,Me dpp})}_3]$.

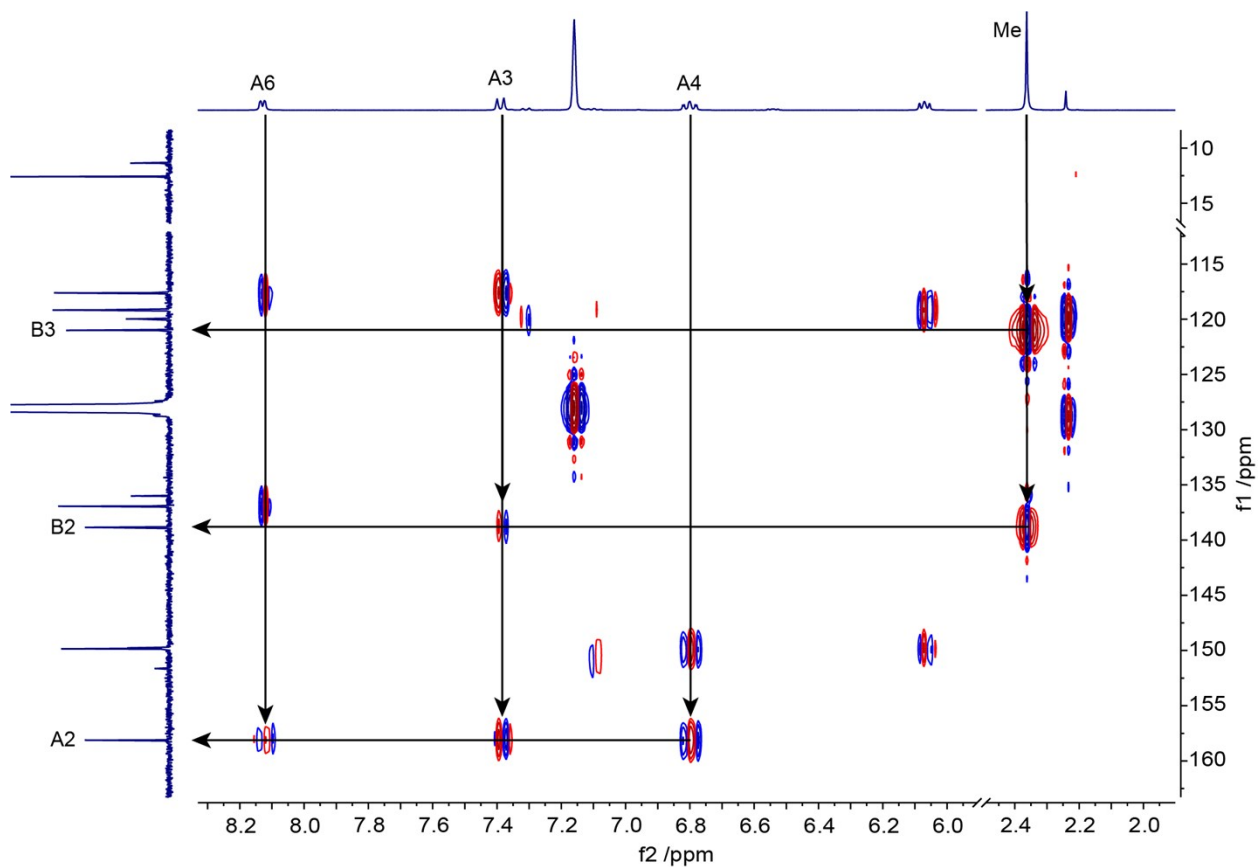


Fig S9. ^1H - $^{13}\text{C}\{^1\text{H}\}$ HMBC NMR (400 MHz, 101 MHz, C_6D_6) spectrum of $[\text{La}(\text{Me,Me)dpp}]_3$.

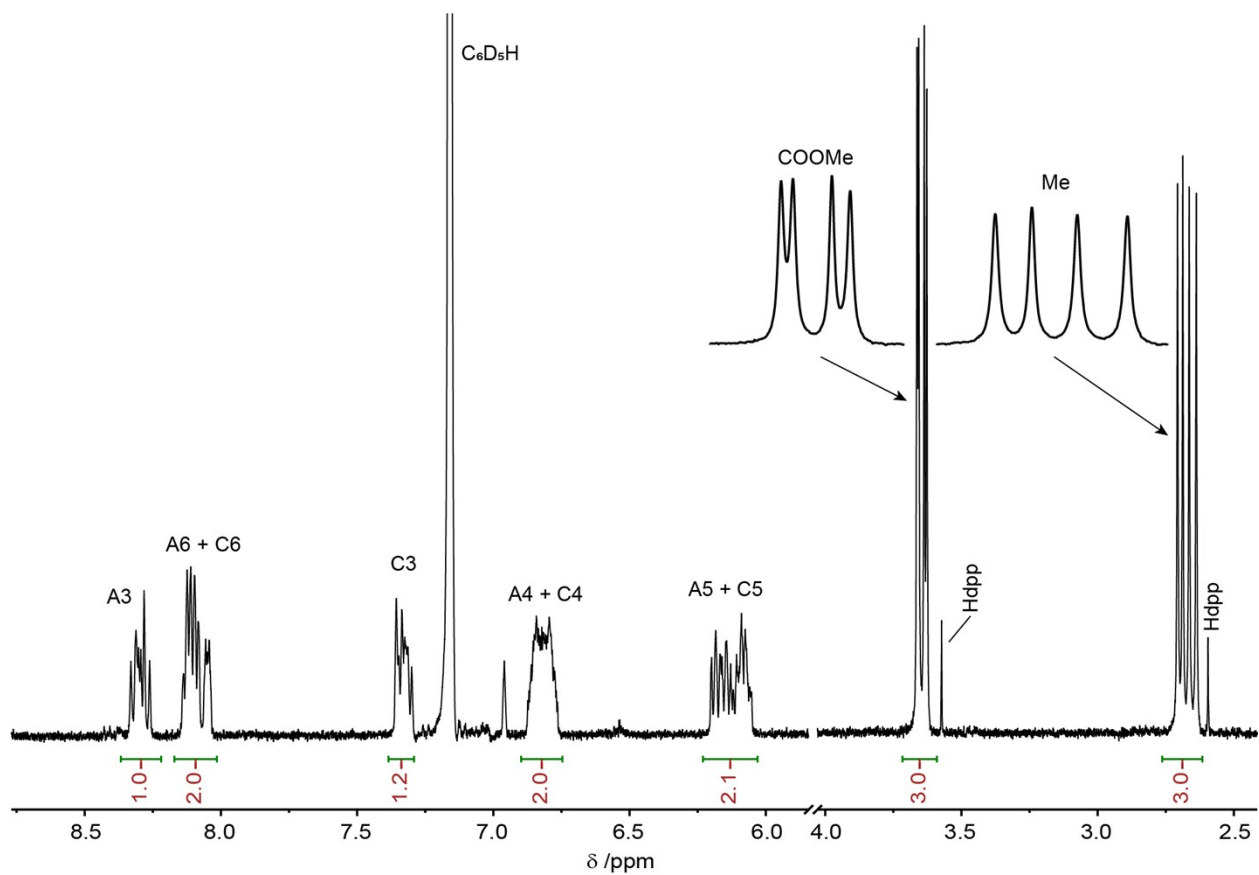


Fig S10. ^1H NMR (400 MHz, C_6D_6) spectrum of $[\text{La}(\text{dpp}^{\text{CO}_2\text{Me,Me}})]_3$.

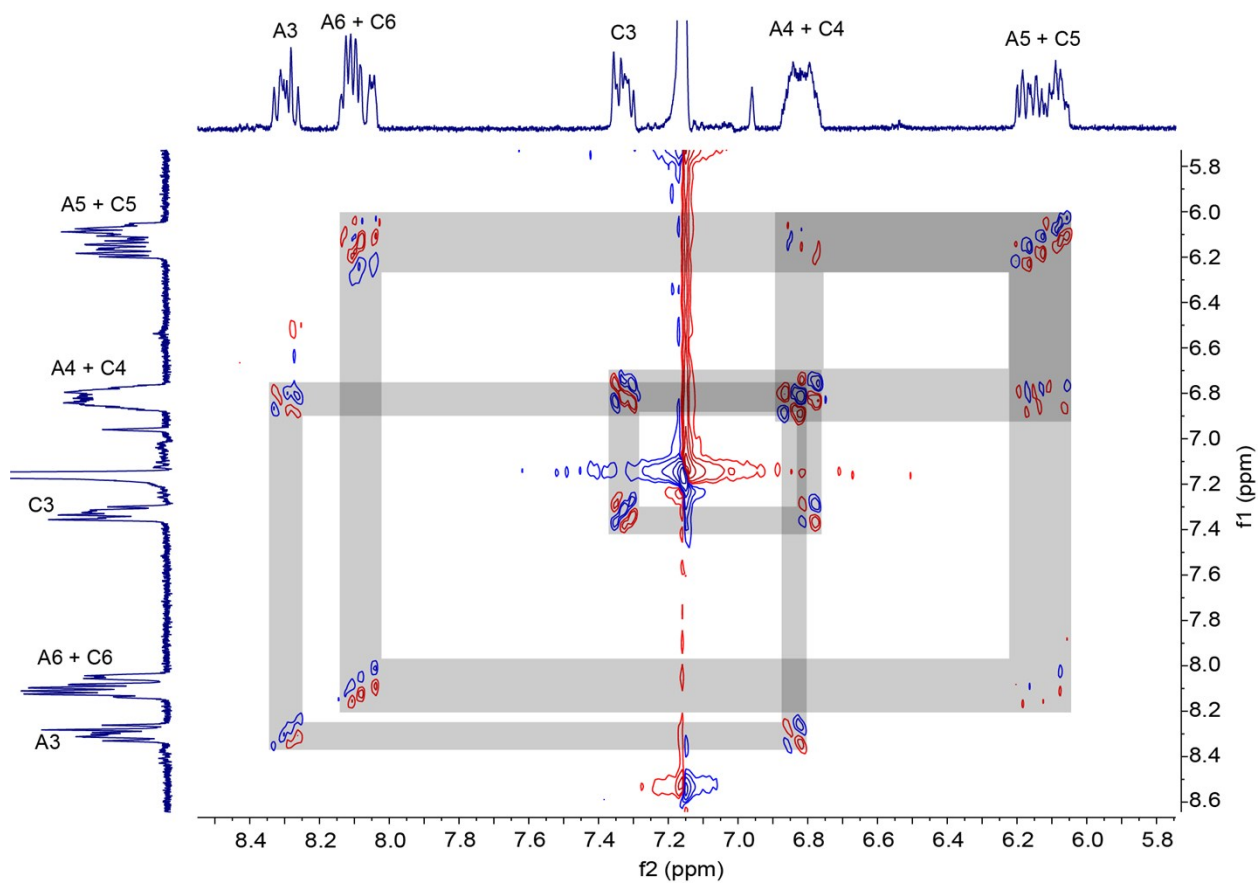


Fig S11. ^1H - ^1H COSY NMR (400 MHz, C_6D_6) spectrum of $[\text{La}(\text{dpp}^{\text{CO}_2\text{Me,Me}})_3]$.

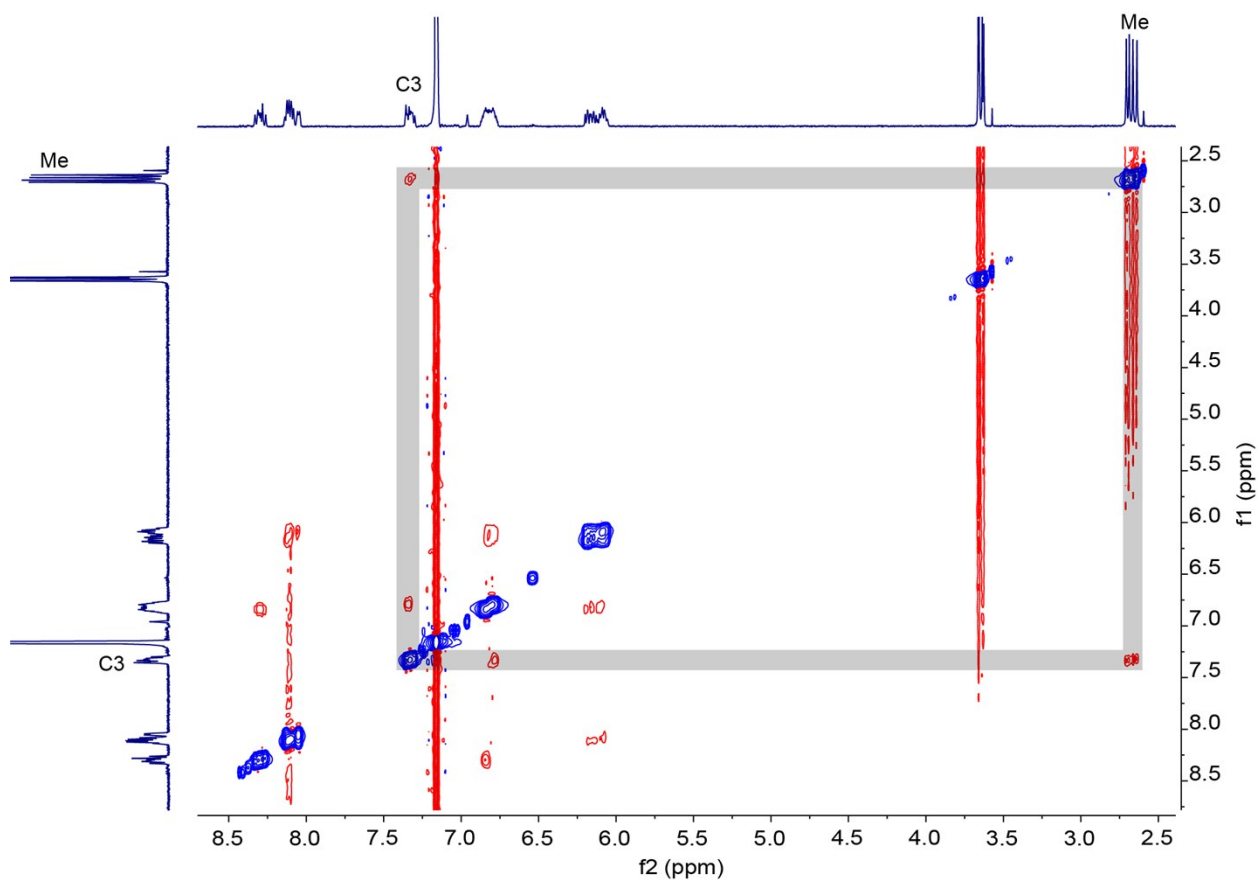


Fig S12. ^1H - ^1H nOeSY NMR (400 MHz, C_6D_6) spectrum of $[\text{La}(\text{dpp}^{\text{CO}_2\text{Me,Me}})_3]$.

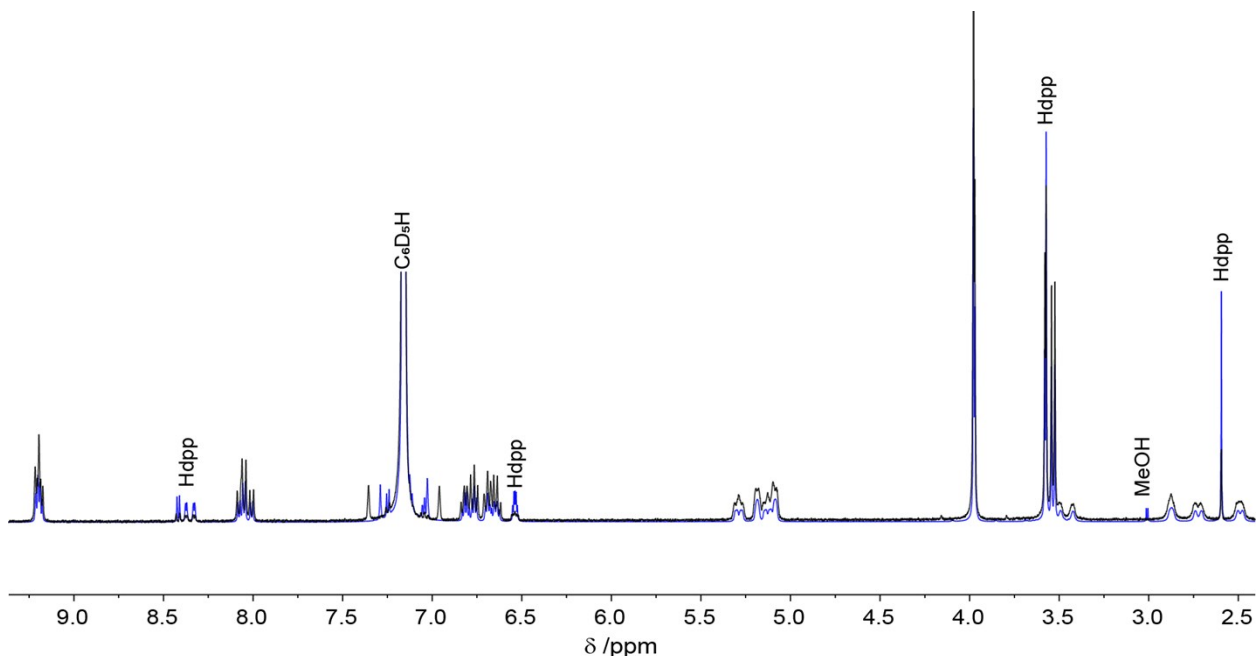


Fig. S13. Superimposed ^1H NMR (C_6D_6) spectra of solutions of $[\text{Sm}(\text{dpp}^{\text{CO}_2\text{Me,Me}})_3]$ prepared separately at different fields (600 MHz in blue, 400 MHz in black).

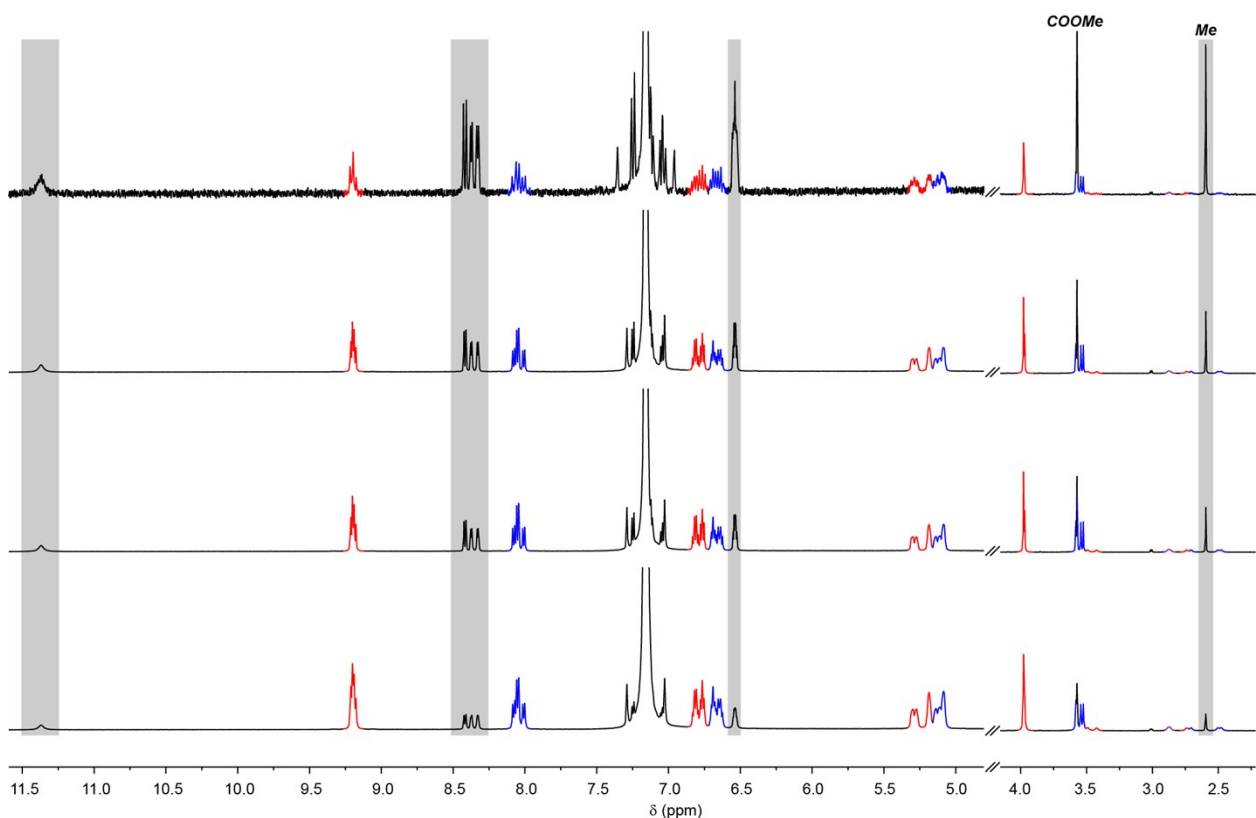


Fig. S14. From bottom to top, ^1H NMR (C_6D_6) spectra of $[\text{Sm}(\text{dpp}^{\text{CO}_2\text{Me,Me}})_3]$: after 20 minutes in solution (600 MHz, bottom), $[\text{Sm}(\text{dpp}^{\text{CO}_2\text{Me,Me}})_3]$ after 4 hours in solution (600 MHz, second from the bottom), after 12 hours in solution (600 MHz, second from the top); and after 9 days in solution (400 MHz, top). Selected signals, which correspond to unbound $\text{Hdpp}^{\text{CO}_2\text{Me,Me}}$ and increase over time, have been highlighted by grey regions, while the signals assigned to the $[\text{Sm}(\text{dpp}^{\text{CO}_2\text{Me,Me}})_3]$ complex (and decrease over time) are coloured red and blue according to their assignment (Fig. X) for clarity. Note – a break in scale occurs between 4–5 ppm.

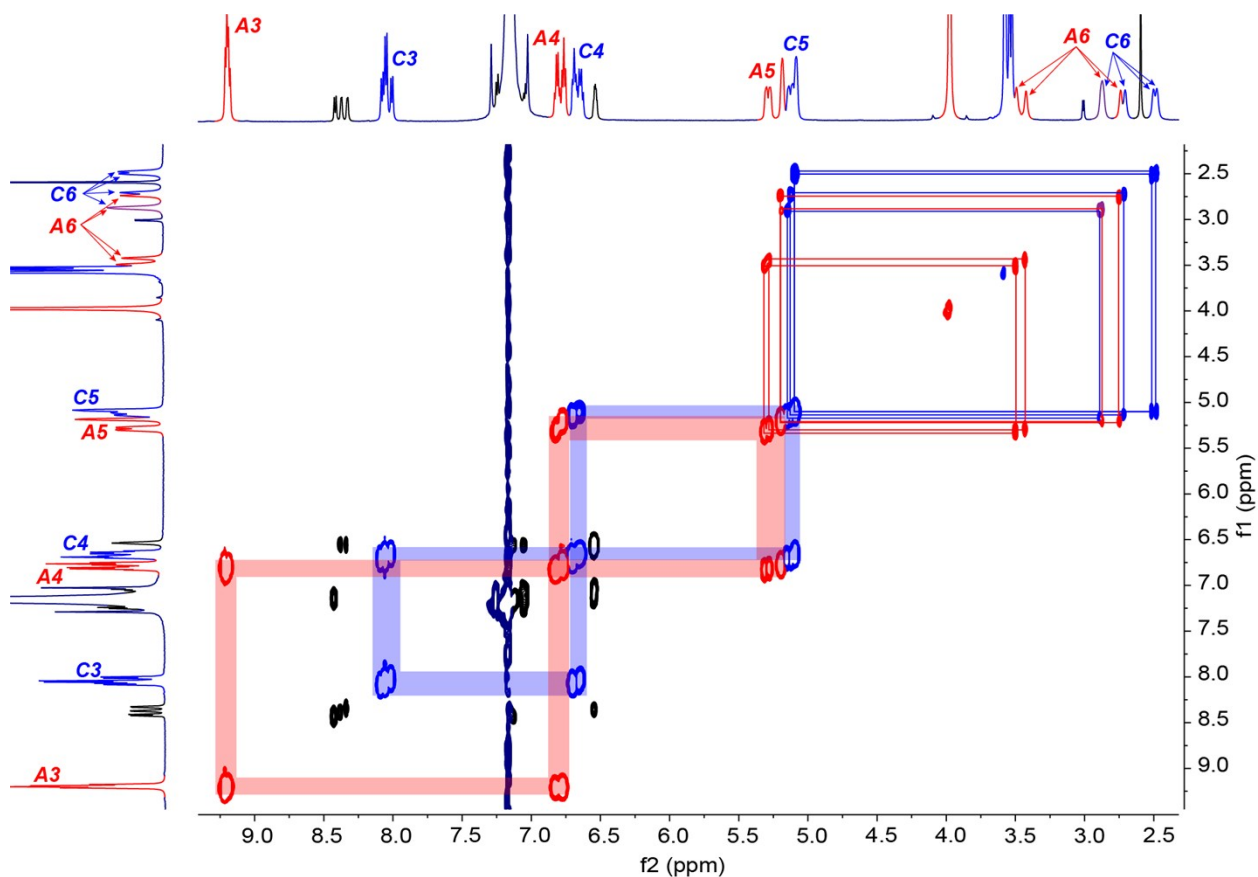


Fig. S15. ^1H - ^1H COSY NMR (600 MHz, C_6D_6) of $[\text{Sm}(\text{dpp}^{\text{CO}_2\text{Me,Me}})_3]$. In black are signals corresponding to free $\text{Hdpp}^{\text{CO}_2\text{Me,Me}}$ which has dissociated during the course of the solution state NMR studies.

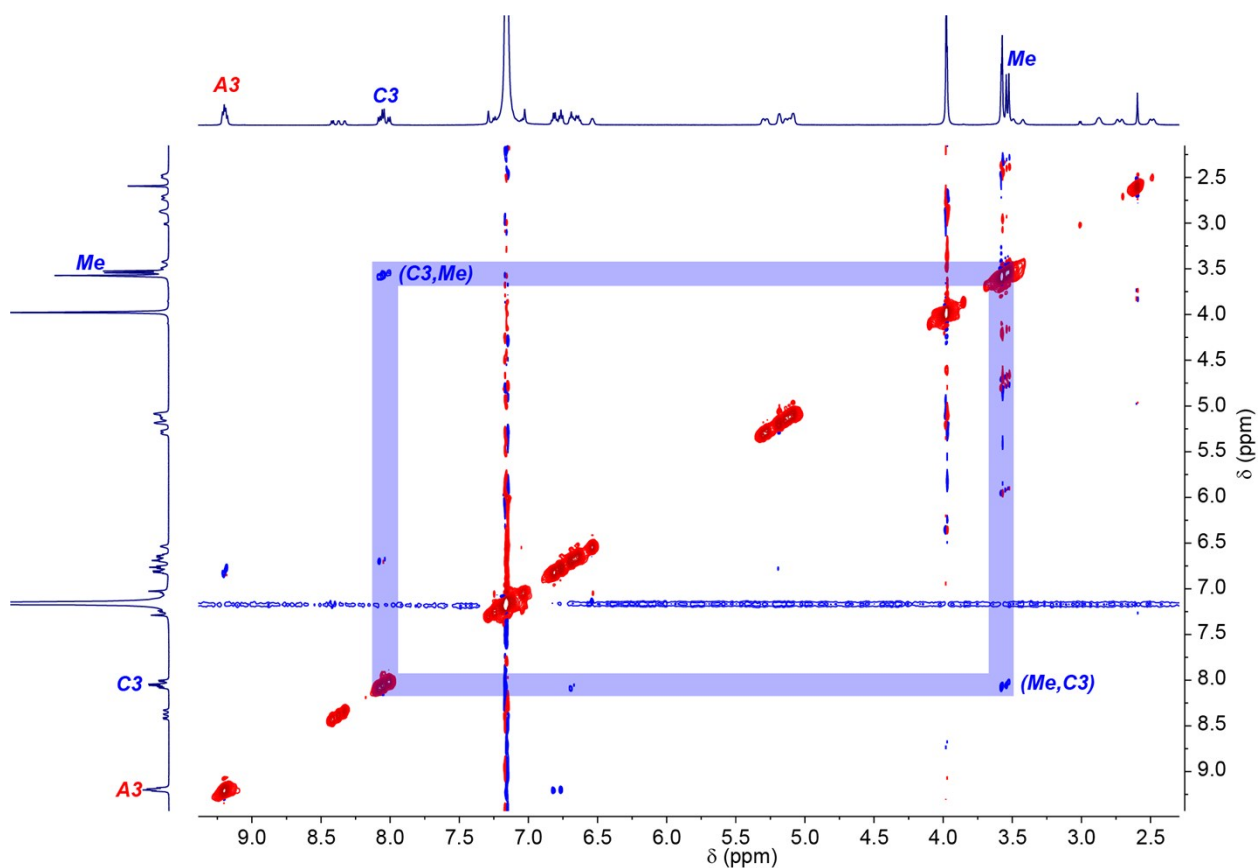


Fig. S16. ^1H - ^1H nOeSY NMR (600 MHz, C_6D_6) of $[\text{Sm}(\text{dpp}^{\text{CO}_2\text{Me,Me}})_3]$ highlighting the key nOe interactions (opposite phase to diagonal peaks) between C3 and the 4-methyl pyrrolide proton environments.

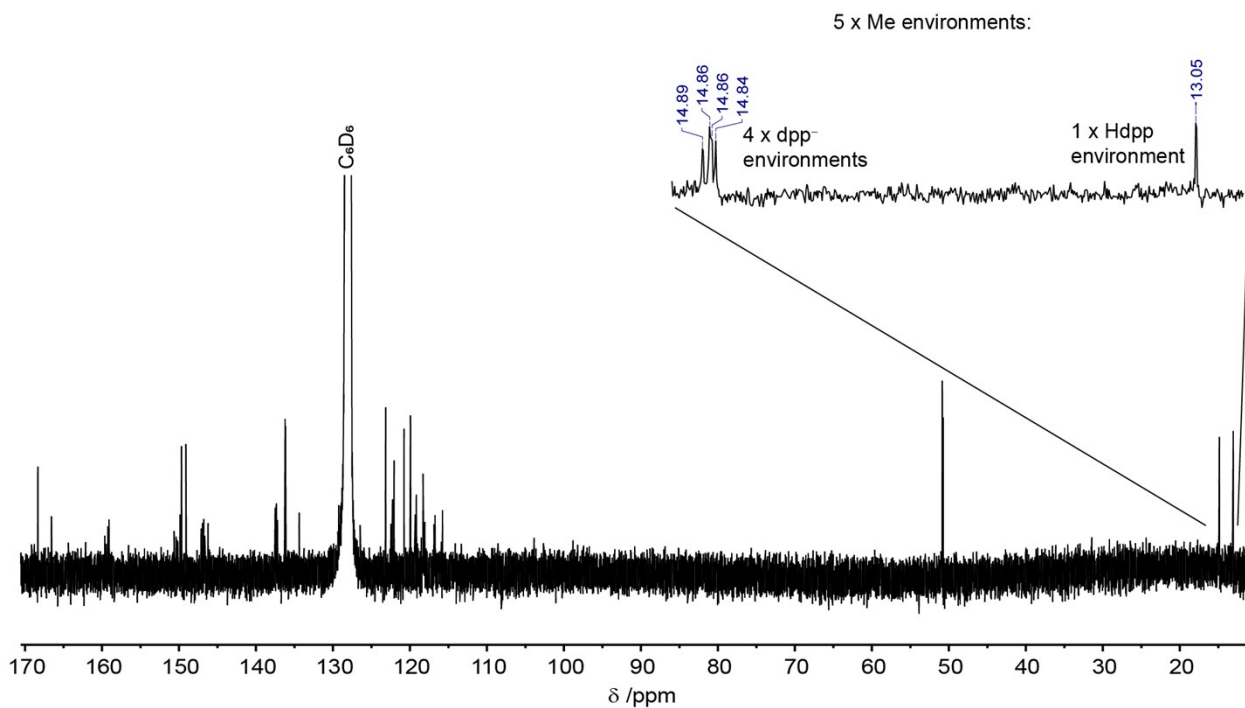


Fig. S17. $^{13}\text{C}\{^1\text{H}\}$ NMR (151 MHz, C_6D_6) spectrum for $[\text{Sm}(\text{dpp}^{\text{CO}_2\text{Me,Me}})_3]$. Shown inset are the five ^{13}C environments associated with the pyrrole methyl substituent.

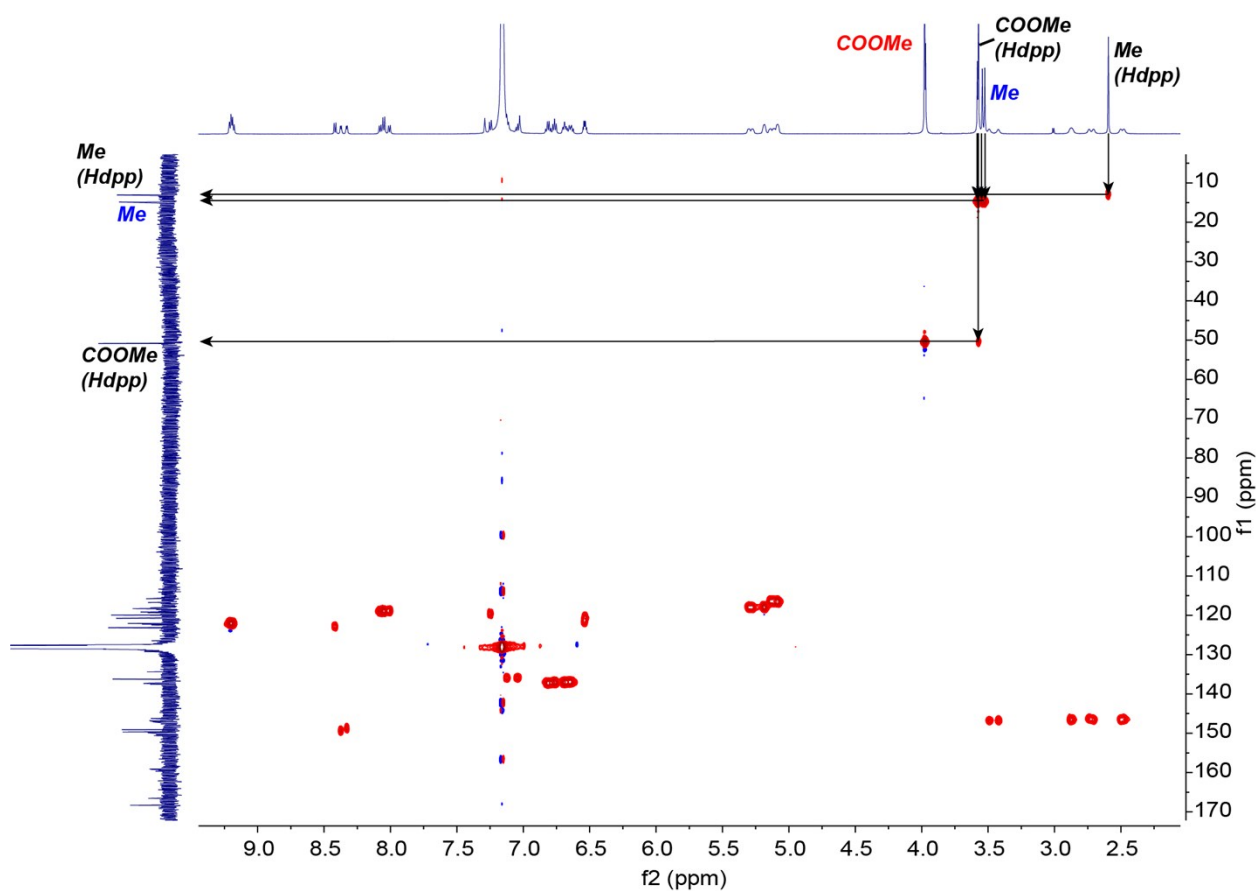


Fig. S18. ^1H - ^{13}C HSQC NMR (600 MHz, 151 MHz, C_6D_6) spectrum of $[\text{Sm}(\text{dpp}^{\text{CO}_2\text{Me,Me}})_3]$.

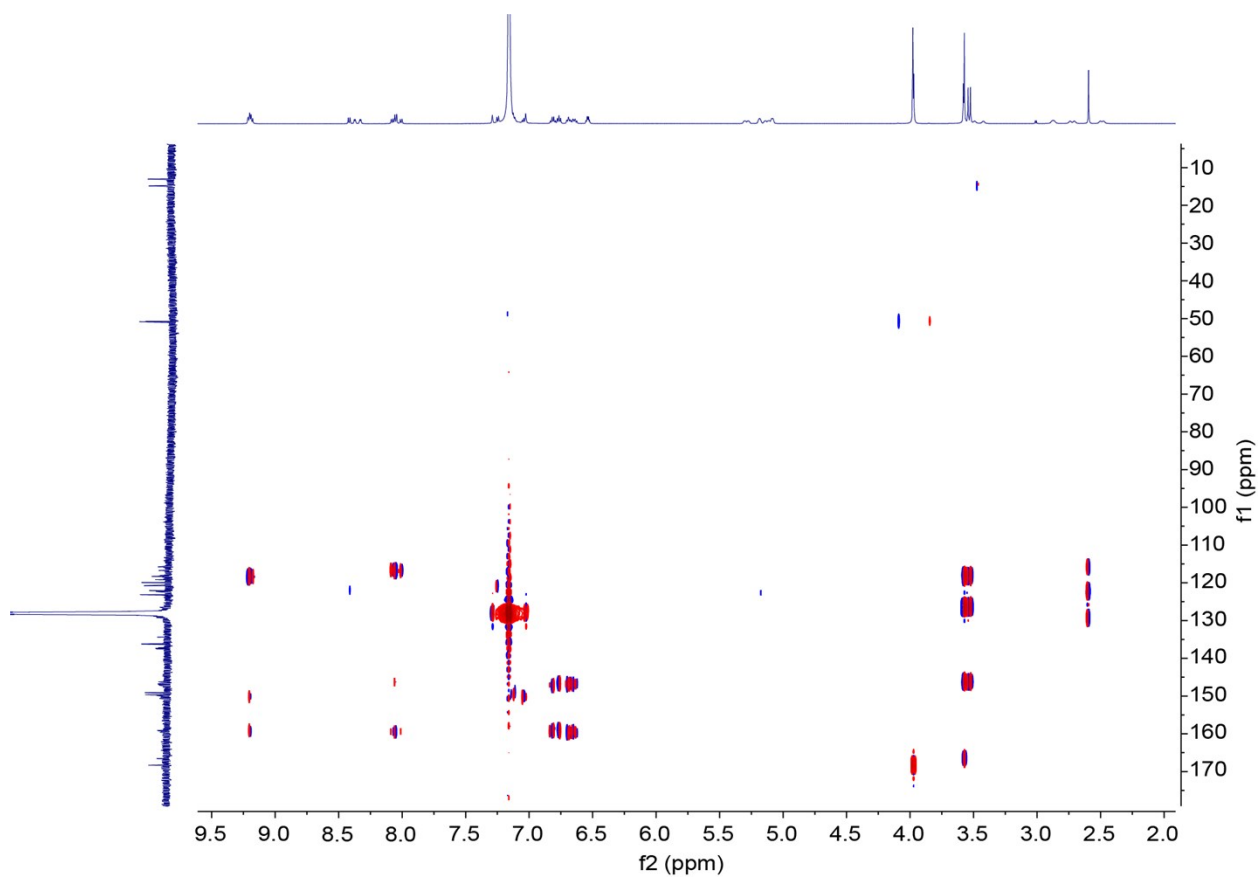


Fig. S19. ^1H - ^{13}C HMBC NMR (600 MHz, 151 MHz, C_6D_6) spectrum of $[\text{Sm}(\text{dpp}^{\text{CO}_2\text{Me,Me}})_3]$.

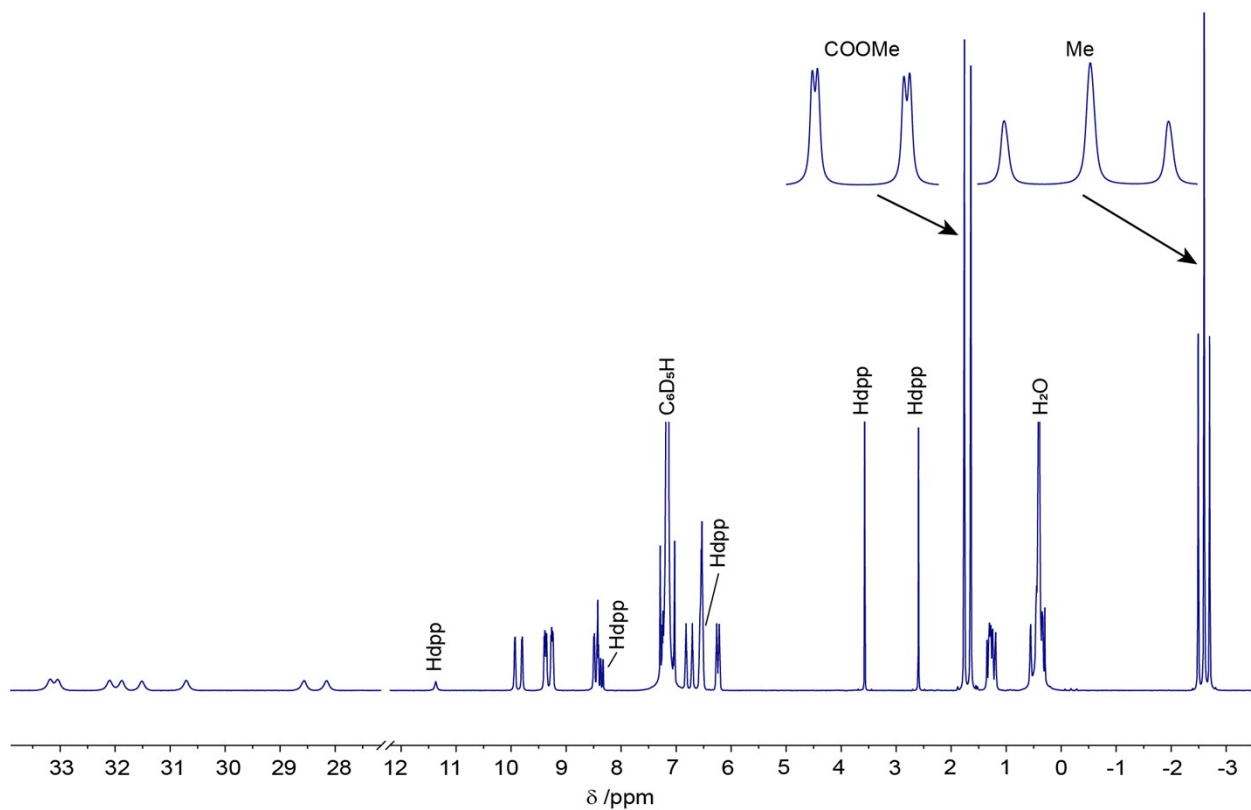


Fig. S20. ^1H NMR (400 MHz, C_6D_6) spectrum of $[\text{Eu}(\text{dpp}^{\text{CO}_2\text{Me,Me}})_3]$.

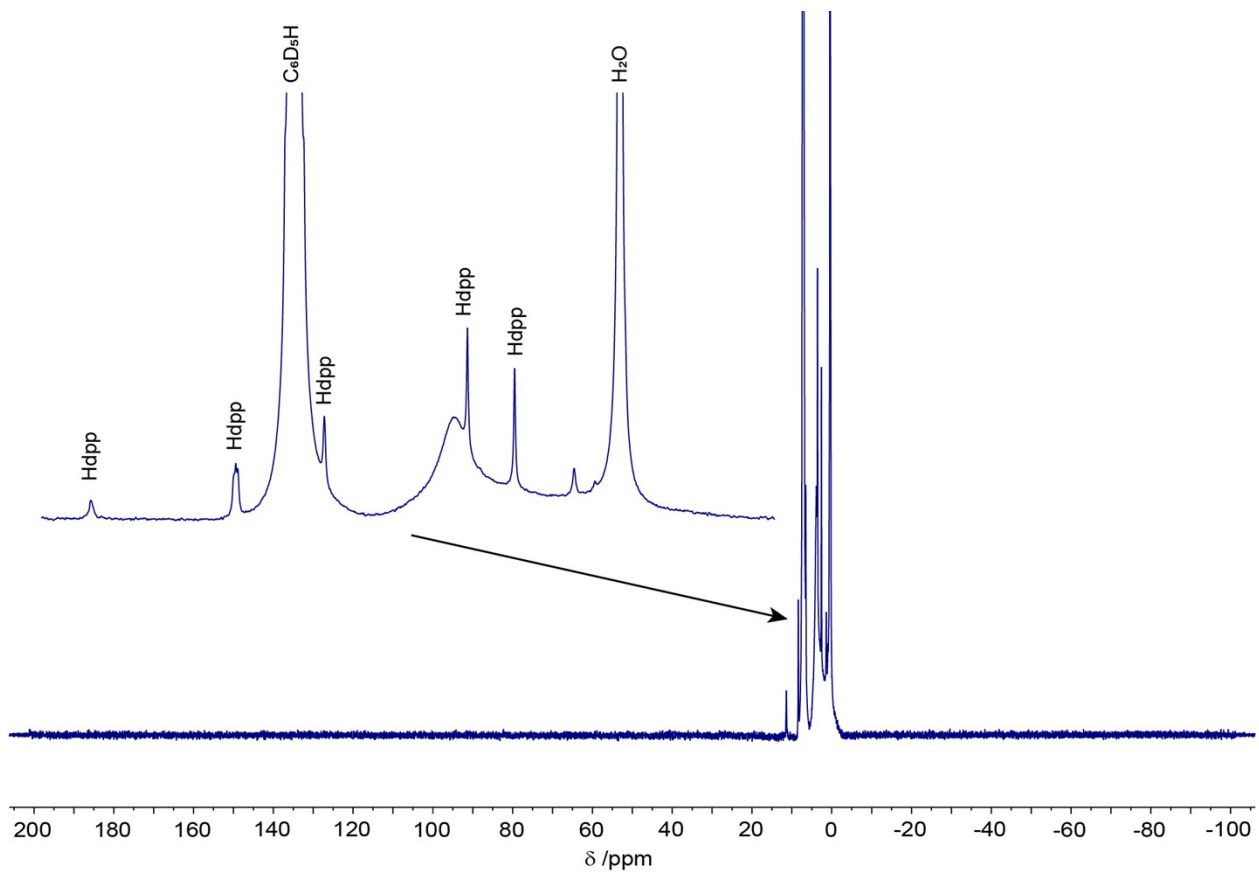


Fig. S21. ^1H NMR (400 MHz, C_6D_6) spectrum of $[\text{Gd}(\text{dpp}^{\text{CO}_2\text{Me,Me}})_3]$.

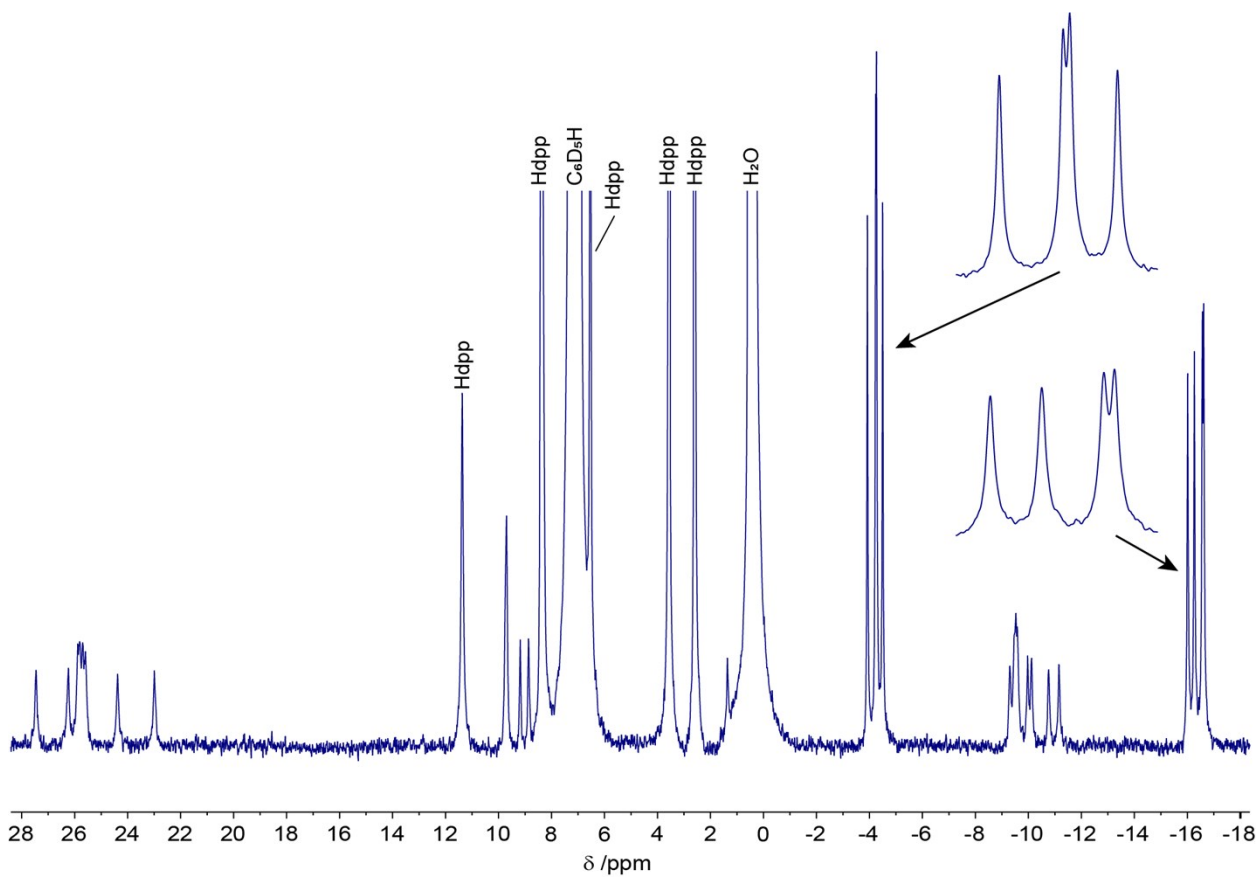


Fig. S22. ^1H NMR (400 MHz, C_6D_6) spectrum of $[\text{Yb}(\text{dpp}^{\text{CO}_2\text{Me,Me}})_3]$.

Mass Spectra

JM-2-19-1 #1-35 RT: 0.01-1.00 AV: 35 NL: 1.99E8
T: FTMS + c NSI Full ms [150.00-2000.00]

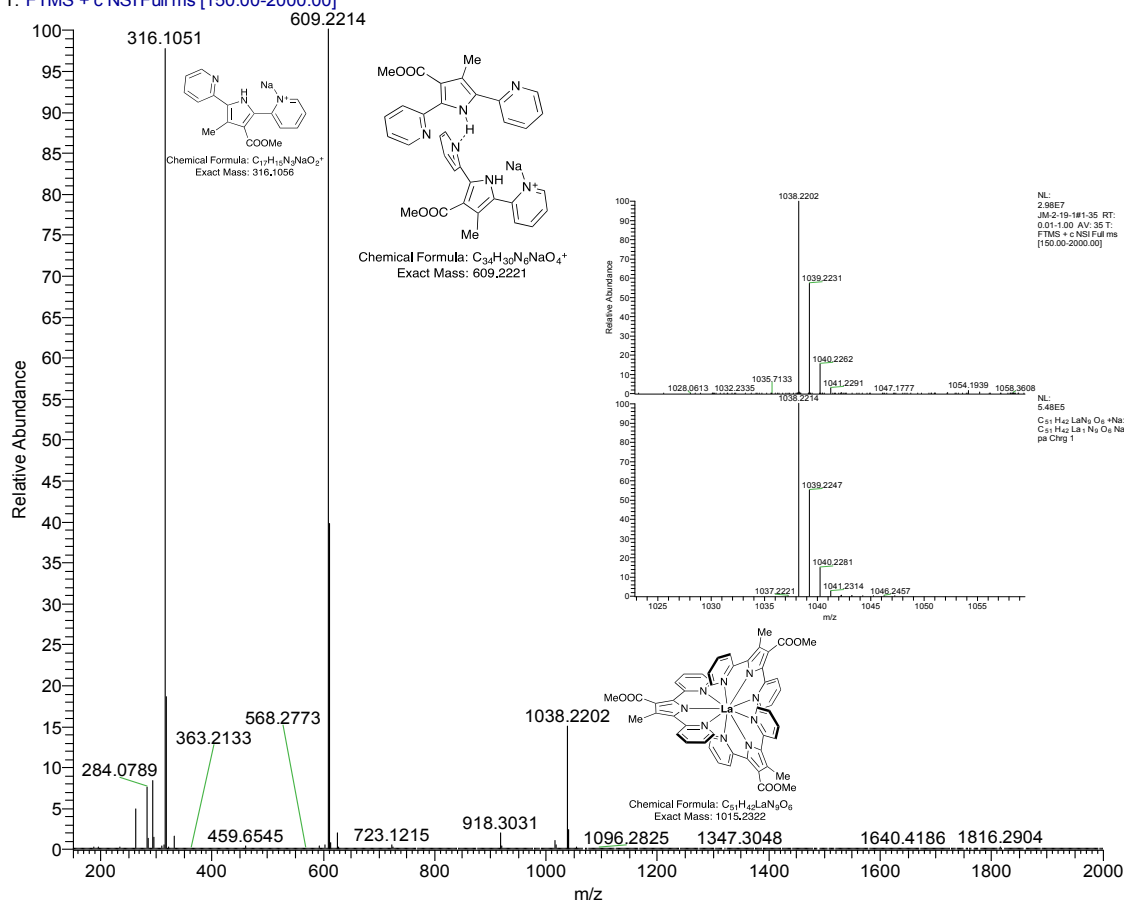


Fig. S23. (+)-HR-NSI-MS of $[La(dpp^{CO_2Me,Me})_3]$ in acetonitrile. Shown inset is the observed isotopomers (top) against the simulated isotopic distribution for $[La(dpp^{CO_2Me,Me})_3 + Na]^+$.

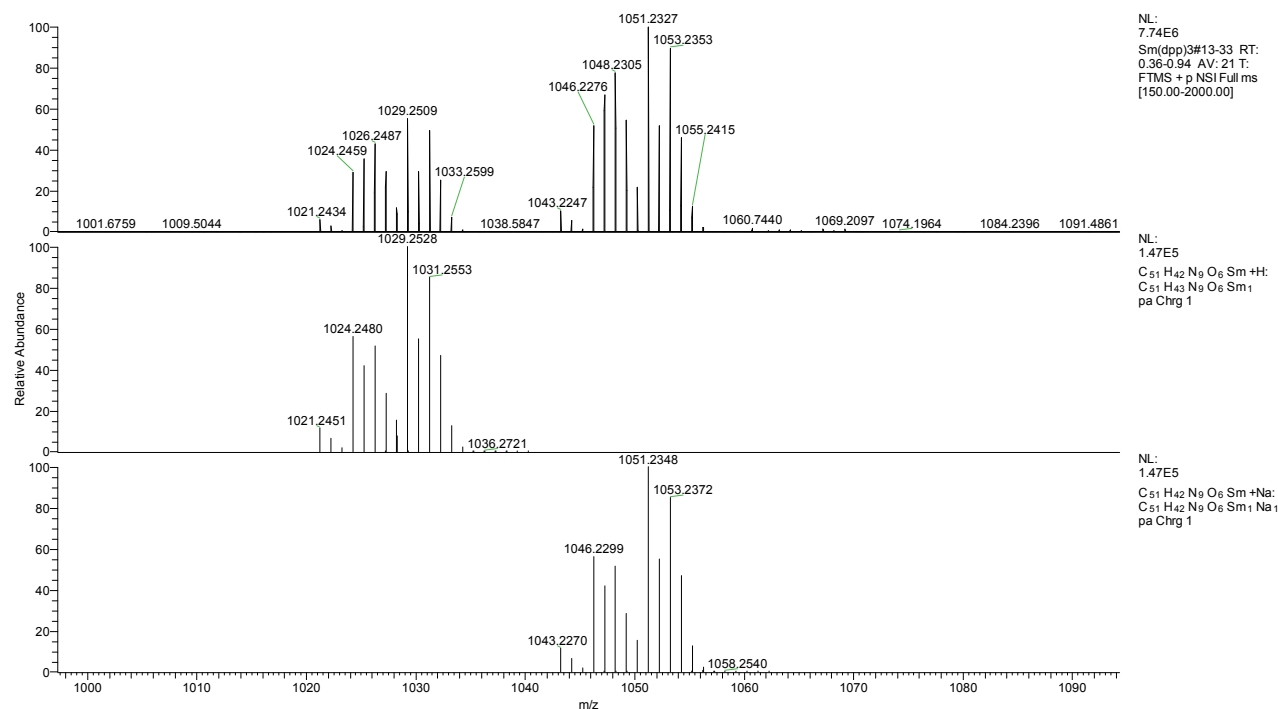


Fig. S24. (+)-HR-NSI-MS of $[Sm(dpp^{CO_2Me,Me})_3]$ in acetonitrile (top), against the simulated isotopic distribution for $[Sm(dpp^{CO_2Me,Me})_3 + H]^+$ (middle) and $[Sm(dpp^{CO_2Me,Me})_3 + Na]^+$ (bottom).

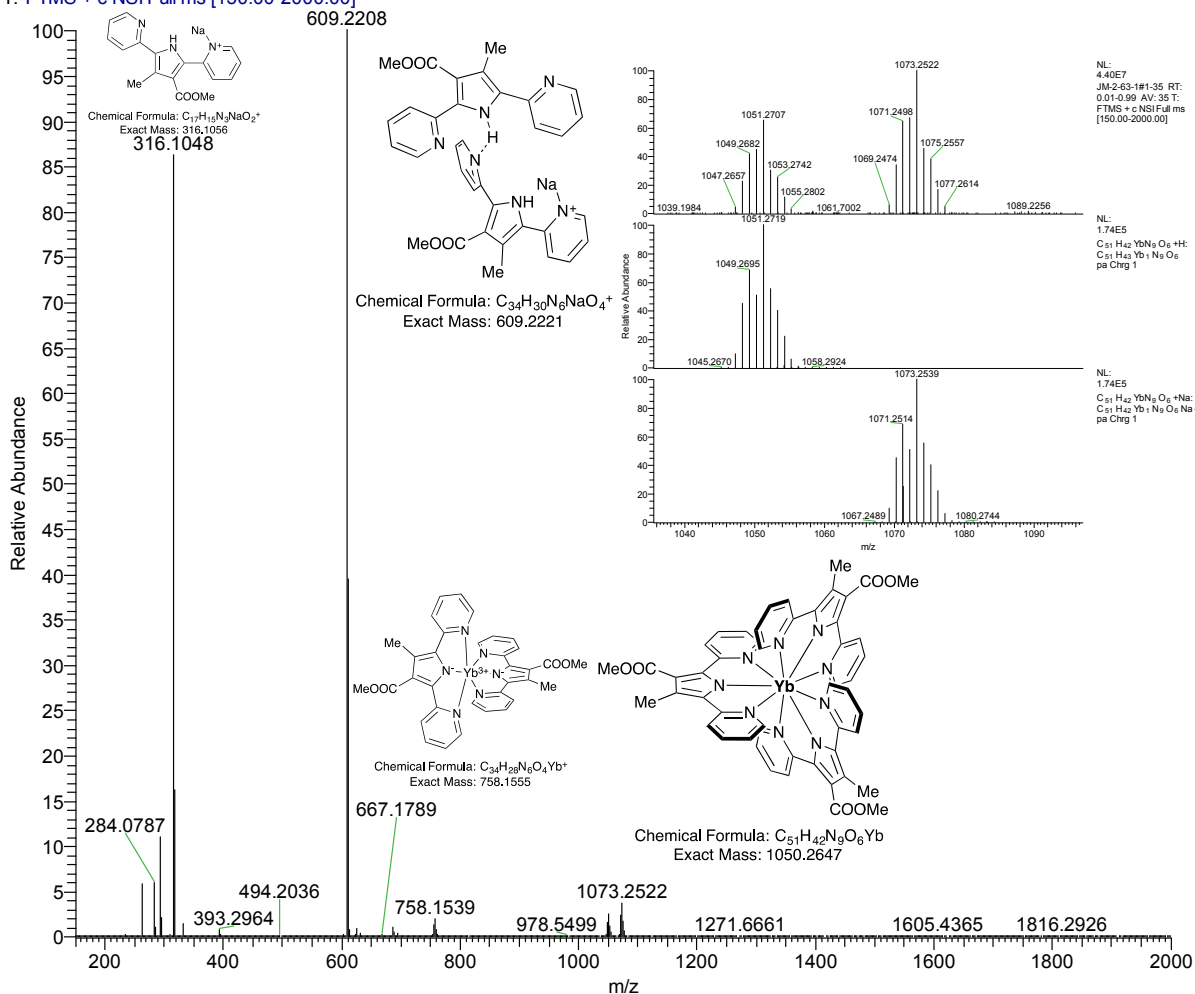


Fig. S25. (+)-HR-NSI-MS of $[Yb(dpp^{CO_2Me,Me})_3]$ in acetonitrile. Shown inset is the observed isotopomers (top) against the simulated isotopic distribution for $[Yb(dpp^{CO_2Me,Me})_3 + H]^+$ (middle) and for $[Yb(dpp^{CO_2Me,Me})_3 + Na]^+$ (bottom).

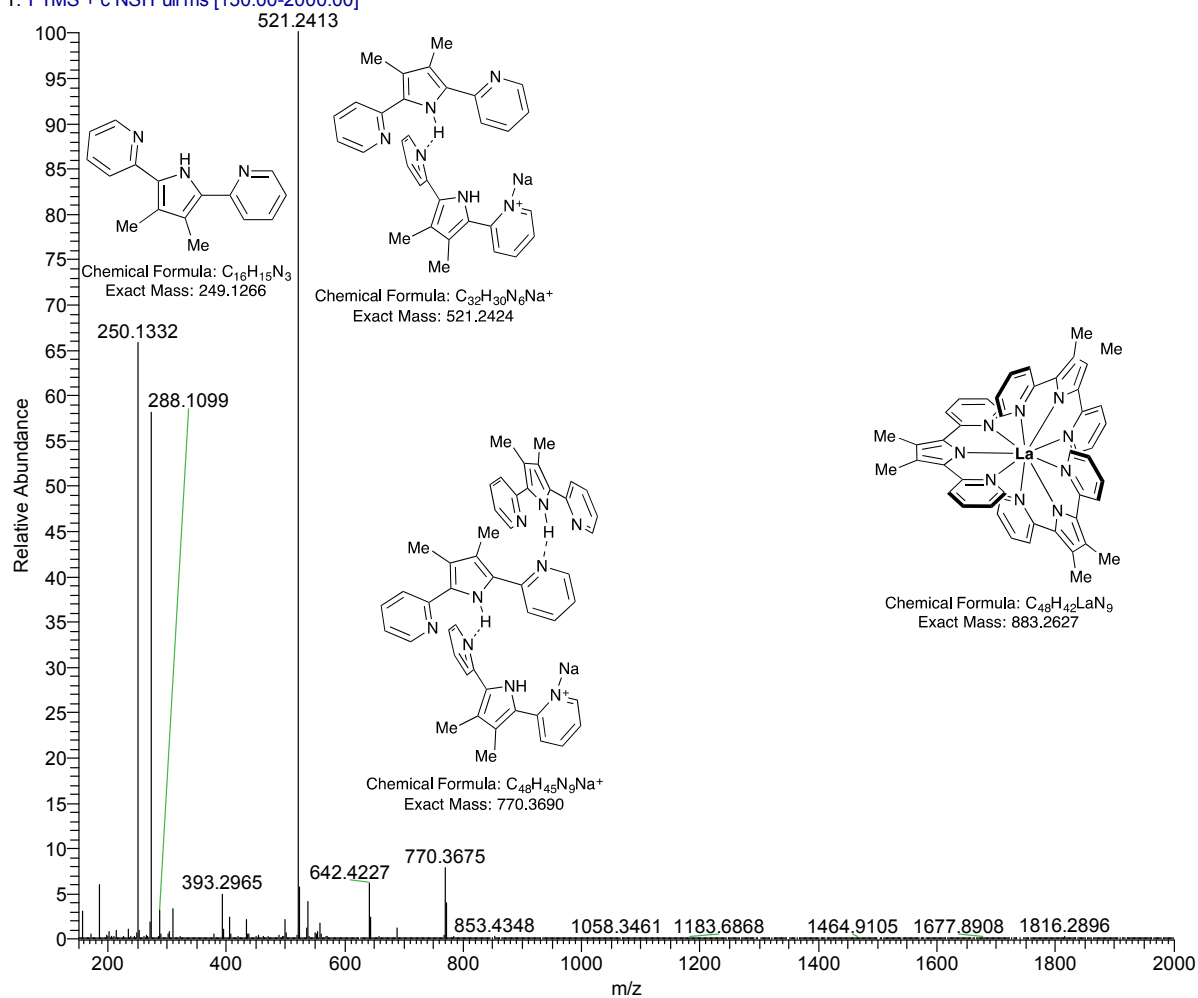


Fig. S26. (+)-HR-NSI-MS of $[La(dpp^{Me,Me})_3]$ in acetonitrile.

Photophysical studies

[Eu(dpp)₃]:

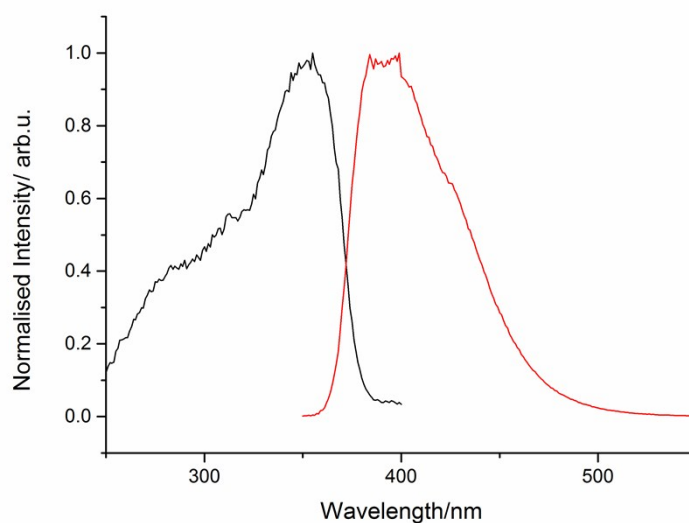


Fig. S27. Normalised excitation ($\lambda_{em} = 612$ nm) and emission ($\lambda_{exc} = 300$ nm) spectra of [Eu(dpp)₃] in CH₂Cl₂ at room temperature.

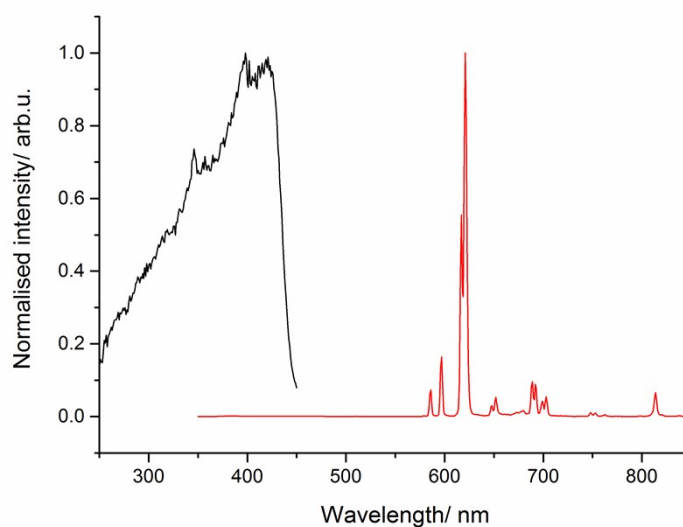


Fig. S28. Normalised excitation ($\lambda_{em} = 612$ nm) and emission ($\lambda_{exc} = 300$ nm) spectra of [Eu(dpp)₃] in CH₂Cl₂ at 77K.

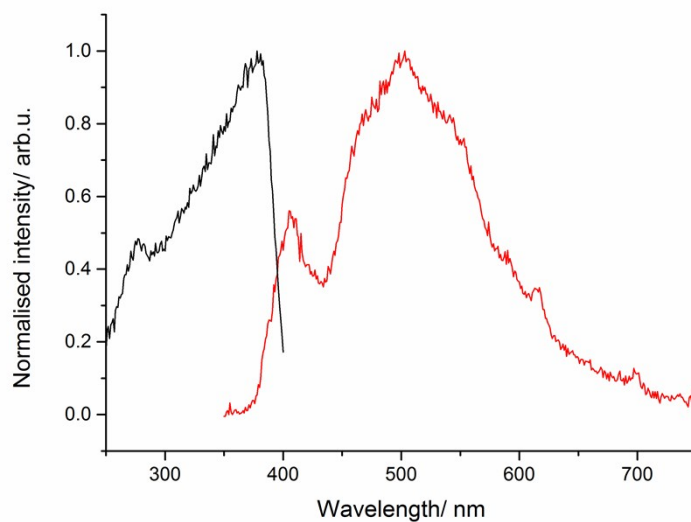


Fig. S29. Normalised excitation ($\lambda_{em} = 612 \text{ nm}$) and emission ($\lambda_{exc} = 300 \text{ nm}$) spectra of $[\text{Eu}(\text{dpp})_3]$ in the solid state.

$[\text{Yb}(\text{dpp})_3]$:

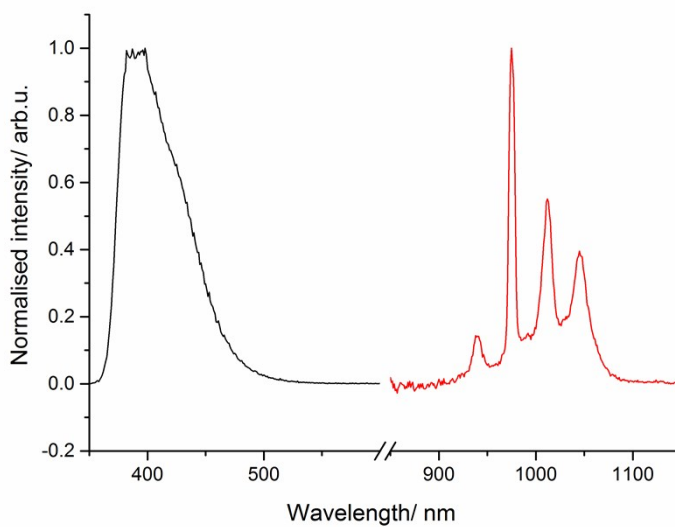


Fig. S30. Normalised excitation ($\lambda_{em} = 980 \text{ nm}$) and emission ($\lambda_{exc} = 300 \text{ nm}$) spectra of $[\text{Yb}(\text{dpp})_3]$ in CH_2Cl_2 at room temperature.

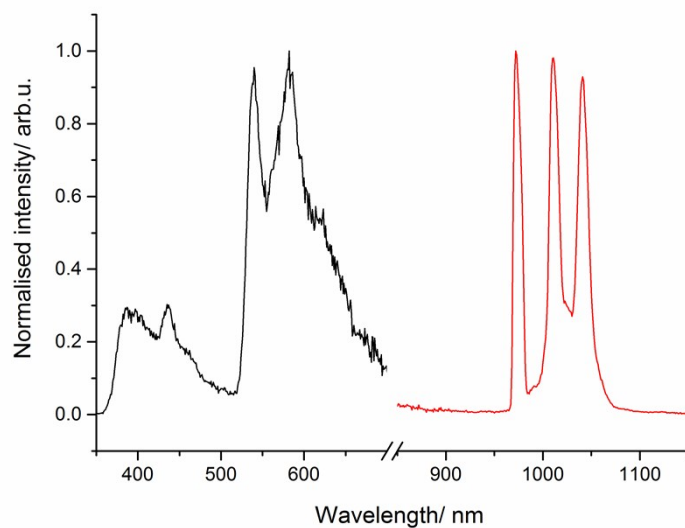


Fig. S31. Normalised excitation ($\lambda_{em} = 980$ nm) and emission ($\lambda_{exc} = 300$ nm) spectra of $[Yb(dpp)_3]$ in CH_2Cl_2 at 77K.

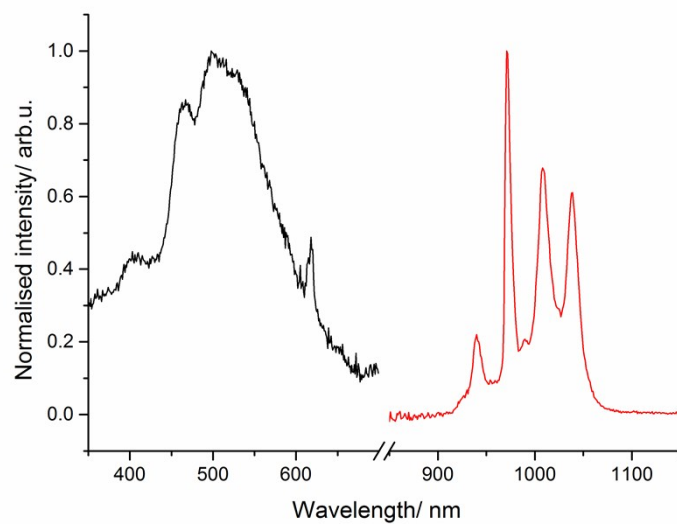


Fig. S32. Normalised excitation ($\lambda_{em} = 980$ nm) and emission ($\lambda_{exc} = 300$ nm) spectra of $[Yb(dpp)_3]$ in the solid state.

Cyclic Voltammetry

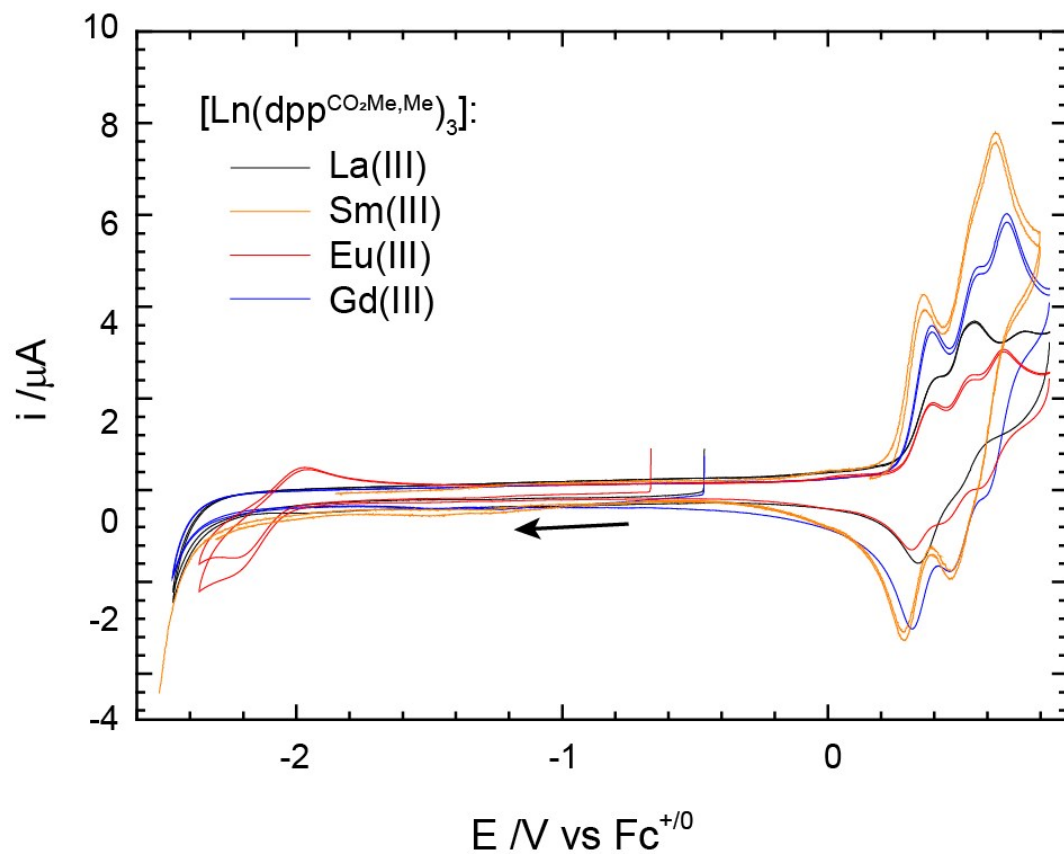


Fig. S33. Overlay of CVs for $[\text{Ln}(\text{dpp}^{\text{CO}_2\text{Me},\text{Me}})_3]$ (Ln = La(III), black trace; Sm(III), orange trace; Eu(III), red trace; and Gd(III), blue trace).

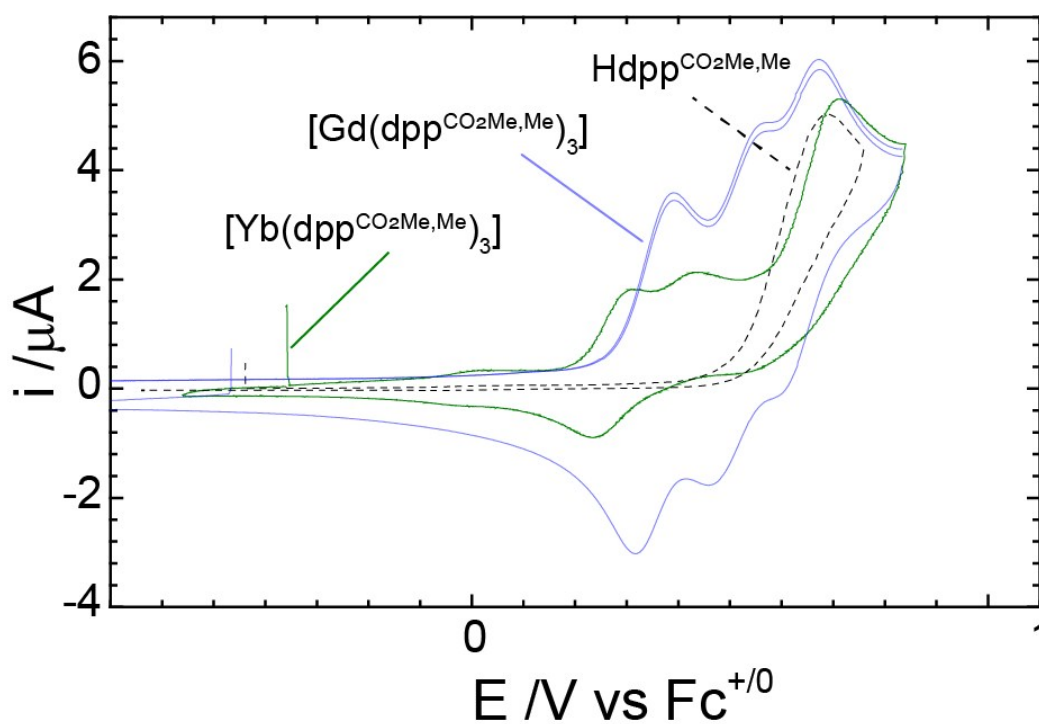


Fig. S34. CV of $[\text{Yb}(\text{dpp}^{\text{CO}_2\text{Me},\text{Me}})_3]$ (green trace) overlaid onto those for $[\text{Gd}(\text{dpp}^{\text{CO}_2\text{Me},\text{Me}})_3]$ (transparent blue trace) and $\text{Hdpp}^{\text{CO}_2\text{Me},\text{Me}}$ (dashed black trace).